Int J Fract
DOI 10.1007/s10704-009-9313-z

ORIGINAL PAPER

Automatic 3-D crack propagation calculations: a pure hexahedral element approach versus a combined element approach

Daniel Bremberg · **Guido Dhondt**

Received: 4 April 2008 / Accepted: 14 January 2009

Abstract This article presents an evaluation of two different crack prediction approaches based on a comparison of the stress intensity factor distribution for three example problems. A single edge notch specimen and a quarter circular corner crack specimen subjected to shear displacements and a three point bend specimen with a crack inclined to the mid-plane are examined. The stress intensity factors are determined from the singular stress field close to the crack front. Two different fracture criteria are adopted for the calculation of an equivalent stress intensity factor and crack deflection angle. The stress intensity factor distributions for both numerical methods agree well to available reference solutions. Deviations are recorded at crack front locations near the free surface probably due to global contraction effects and the twisting behaviour of the crack front. Crack propagation calculations for the three point bending specimen give results that satisfy intuitive expectations. The outcome of the study encourages further pursuit of a crack propagation tool based on a combination of elements.

D. Bremberg (✉)
Department of Solid Mechanics, Royal Institute of Technology (KTH), Osquars Backe 1, 100 44 Stockholm, Sweden
e-mail: bremberg@kth.se

D. Bremberg · G. Dhondt
MTU Aero Engines GmbH, Postfach 50 06 40, 80976 Munich, Germany

Keywords Linear elastic fracture mechanics · Finite element method · Crack growth · Mixed mode · Stress intensity factor

1 Introduction

In recent years it has become evident that the increasing performance requirements for many industrial applications demand ever more accurate analyses at an early stage of development. An example of such an area is the field of aero engines. New requirements that set high standards concerning high temperatures, low weight and cost efficiency lead to the need for new tools to meet these requirements. To further stress the importance of new tools, the increasing ability of component design that brings a wider range of complex loading scenarios is worth mentioning. All these ingredients have to be considered during the development phase. One aspect of design is the risk of crack nucleation and subsequent crack propagation. Assuming the crack is already present, the task may be to investigate whether or not the introduced crack constitutes a risk.

To instigate a crack growth analysis a geometrical model, the complete loading, material parameters and crack propagation data are needed. In most practical situations, the geometrical model, the loading and material parameters are probably already at hand. Other type of data such as fracture parameters and crack descriptions may vary depending on which crack propagation software is used.

Most crack propagation tools are based on the frameworks of the finite element method (FEM) (Zienkiewicz 1971) as well as the boundary element method (BEM) (Brebbia 1978). The BEM reduces the number of meshing operations since only the surface representation is involved. It brings the big advantage that the complexity of meshing the complete structure is eliminated. However, the underlying theory is more difficult to grasp and the FEM has therefore gained more ground in the industry.

There are a number of crack propagation tools available, some have already been incorporated into commercial software while others are intended for academic purposes. An investigation of existing numerical approaches (Riddell et al. 1997) compares two categories of software. The first category includes methods based on libraries of stress intensity factor (SIF) solutions for a variety of crack configurations, e.g. NASA/FLAGRO (Forman 1988) and NASCRAC (1989). A process relying on libraries may lead to significant deviations in the results if the analysis extends beyond the available libraries. The second method investigated, the BEM-code FRANC3D (Wawrzynek et al. 1988), is based on an evaluation of the crack growth from point SIFs. Allowing the crack to grow according to the results in each point, the crack is no longer constrained to trail empirical results. The conclusion drawn from these comparisons is that FRANC3D requires considerably longer computational times but has a major advantage in cases where the libraries are not sufficient.

Most crack propagation software used in the present days have abandoned the library based approach. Zencrack (Timbrell and Cook 1997) uses a method bases on a pure hexahedral mesh. A remeshing and splitting procedure applied to so-called crack blocks allows the crack to grow out of plane. Results look promising but the input mesh must consist of hexahedral elements. ADAPCRACK3D (Schöllmann et al. 2003) is a FEM-code that makes use of a sub modelling technique. The global mesh consists of a pure tetrahedral mesh where the crack is easily taken into account due to the element properties. The resulting FE-solution is then mapped to the sub model consisting of only hexahedral elements. Crack propagation is calculated based solely on the subsequent FE results from the sub model computations. The use of a modified BEM, the dual boundary element method (DBEM), for crack propagation evaluations has been investigated in the past (Mi and Aliabadi 1992; Cicilino and Aliabadi 1999). A more recent evaluation that includes a comparison of the FEM-code ADAPCRACK3D and the DBEM-code BEASY (2007) reveals that both the FEM and the DBEM give results that correspond well to the existing experimental findings (Citarella and Buchholz 2008). The above considerations have led to the belief that a crack propagation tool within the framework of FEM ought to be pursued.

Developing a crack propagation tool raises many questions regarding the approach. Several aspects have to be taken into account and fundamental requirements have to be met. One such requirement is the ability to treat non-planar crack growth in three dimensions. Automation turns out to be very important as the analysis is an incremental process and little user intervention is desirable. There is clearly no need to develop a tool that does not return accurate results. The main problem combining crack propagation calculations and FEM is the insertion of the crack into the mesh at hand. Performing the task of inserting a crack configuration into an arbitrary mesh is challenging. Some software solves this difficulty by letting the crack growth remain in one plane. Our intuition tells us that there are few real life examples where such an assumption is fulfilled. The wish for an automatic tool sets high expectations on the meshing capabilities. Due to this, not all element types can be used. It is for instance well established that the task of meshing an arbitrary geometry with brick elements is not feasible. Attempts have been made but it has proven very difficult. Automatic meshing of structures requires the use of tetrahedral elements which are better suited for mesh generation. This fact has opened up for other more sophisticated methods including, for instance the sub-modelling technique, where the use of a combination of mesh types has been investigated. The approach requires that the FE-program can deal with sub-modelling and that two computations are being performed, one for the global model and one for the sub-model. It has become clear that it is not sufficient to use only one element type in order to alleviate the problems that arise. At the same time, if external software is relied on it should be as generic as possible.

The idea has evolved to develop a method that makes use of a combination of elements. It is expected that the proper combination of elements can yield accurate crack propagation calculations and versatile meshing capabilities simultaneously. A concentric structured mesh consisting of several layers of hexahedral elements enclosing the crack front should provide an appropriate singular representation of the stress field. The remaining part of the structure volume is filled with a tetrahedral mesh. Ending up with two or more separate meshes, these are connected by linear constraint equations.

This article presents a comparison between two different methods used for crack propagation calculations. The first method, the pure element approach, restricts the crack to remain in one plane while the second, the combined element approach, allows the crack to grow arbitrarily. The basic theory and ideas behind the two methods are presented in Sect. 2. Sections 3 and 4 treat the fracture criteria and crack growth law, respectively. The two methods are briefly explained in Sects. 5 and 6. Three example specimens chosen for the investigation are presented in Sect. 7. Section 8 shows the resulting SIF distributions after the first increment for two of the specimens and the crack growth results for a selection from 70 increments for the third specimen are given in Sect. 9. The article is concluded with some final remarks.

2 Collapsed quarter point element stress field

One category of methods available for crack propagation computations are the local methods. It is a type of method where the crack growth is based on the local stress or strain field directly ahead of the crack front. Within the framework of linear elastic fracture mechanics (LEFM), the analytical expressions for each of the three SIFs are commonly expressed as an asymptotic solution consisting of the leading singular term only. Higher order terms vanish as the radius decreases and the non-singular term may be omitted for LEFM applications. This implies that the SIFs can be determined once the stress field in the near region of the crack front has been established. The stress field is determined through the use of any FE-program. A sufficiently accurate stress field can be obtained from the integration points inside the elements. This boils down to the conclusion that the SIFs can be accurately calculated from the integration points of elements able to characterise the asymptotic stress and strain field as defined by the analytical solution.

The best suited element is the so-called collapsed quarter point element as derived in (Dhondt 1993). It is a 20-node brick element that exhibits the necessary singular shape functions required by the asymptotic solution. The correct near-field stress state is achieved by placing such elements concentrically along the crack front. In order to avoid the decision of whether plane strain or plane stress prevails, only the five stress components acting orthogonal to the crack front tangent are considered leaving the three SIFs as unknowns. For each of the two integration points immediately ahead of the crack front, the unknowns are determined by solving a system of five equations for the three unknowns through a least squares computation. The local SIF values are taken as the mean of the two solutions.

3 Fracture criteria

Structures of arbitrary geometry that are subject to thermo-mechanical loads are examples in which crack growth due to mixed-mode loading is inevitable. The simple reason is that the stress field in the near region of the crack front does not correspond to a pure tension loading. Hence, crack growth predictions need criteria that do not account for Mode-I alone. Several concepts that account for Mode-I/Mode-II loading have been developed. There are also criteria that take into account Mode-III although its influence and effect is not entirely clear. Including the third loading mode introduces an additional deflection angle. There are different viewpoints to how this second angle should be defined. However, it is agreed that the angle somehow represents a tilting of the crack front tangent. Since no information is given on how long the tilting stretches, it would be nearly impossible to incorporate the resulting facets into crack propagation software. This phenomenon is therefore left out for the time being. The reader can find more information on different fracture criteria in (Richard et al. 2003).

The pure hexahedral approach uses the minimum strain energy density (SED) criterion by Sih. It includes all three modes of loading and two deflection angles. However, deriving an expression for the minimum SED it can be noted that the dependence of Mode-III and the second deflection angle disappears. In other words, the criterion can be regarded insensitive to Mode-III even though it is included in the basic expression.

A criterion based on the maximum principal stress (MPS) can be found in (Chanel and Dhondt 2007). It is argued that the crack grows in a plane satisfying two criteria:

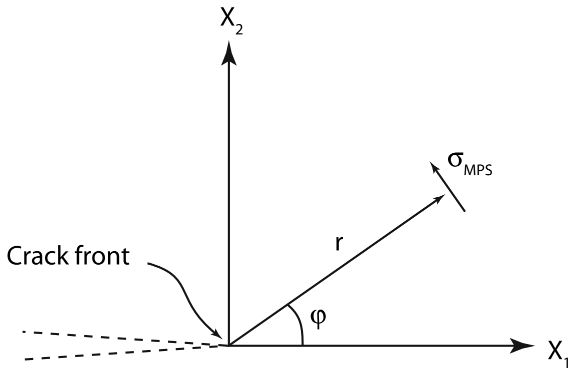

Fig. 1 Local coordinate system defined at the crack front

- The plane contains the crack front, i.e. it is a radial plane
- The plane is a principal stress plane, i.e. there is no shear stress in that plane

If more than one plane satisfies these two criteria, of all the planes satisfying the criteria the one exhibiting the largest normal stress is taken to be the solution. Inherently, the criterion makes the crack growth seek the state of a pure Mode-I loading. An equivalent stress intensity factor is acquired from the self-similar stress based on the largest principal stress and the crack growth direction is given directly from the deflection angle, see Fig. 1.

4 Crack growth law

The crack growth per cycle can be described by the Paris Law (Paris et al. 1961; Paris and Erdogan 1963) under the assumption that the amplitude loading is constant during each cycle. If the assumption is extended to be valid for a finite number of fatigue cycles, the crack growth length for these cycles is calculated based on the crack growth rate in the first cycle.

Using a large number of cycles for each crack growth increment means less increments are needed. On the other hand, too large a number of cycles leads to decreasing accuracy. Such a loss can be expected for instance if the crack growth increment is large enough to extend past a point that would have influenced the crack deflection. It is however not realistic to let the program run for each loading cycle. Instead, it is argued that a good way to govern the crack growth is to prescribe a maximum growth increment and let the number of cycles vary from increment to increment. Even though the crack grows differently along its crack front, allowing the number of load cycles to vary is expected to give a more stable crack growth. The growth rate at any given point is governed by the maximum crack growth rate among all points along the crack front. This means that the crack growth between any two points along the crack front can deviate significantly if the corresponding crack growth rate is different.

5 The pure element approach

Starting point is a mesh consisting of only 3-D 20-node brick elements. Insertion of the crack and its front is performed by the pre-processor. It identifies which brick elements are cut by the crack faces. The free crack surface boundary is generated through division and separation of the cut elements while the mesh at the crack front is replaced by a new structured mesh with collapsed quarter point elements inserted in the direct connection to the crack front. The output is an input mesh used for stress calculations with a generic FE-solver.

From the resulting stress field at the crack front, the stress intensity factors for all three modes of loading (Mode-I, Mode-II and Mode- III) can be determined by a comparison to the analytically described asymptotic stress field. Applying an appropriate crack propagation law, such as the Paris Law, the number of cycles is determined assuming that the stress intensity factors remain constant during all cycles. Once the number of cycles has been determined, the new crack front is calculated and attached to the previous crack description. The incremental process is reinitiated unless the stopping criterion is satisfied.

The program was developed in the mid-nineties and has been used extensively for a variety of real-life engine components. It has proven to be a reliable tool that can take into account sharp edges and notches, something that is rare among other crack propagation software. Since the initial mesh is only slightly modified and most of the reference mesh is kept intact, the algorithm is fast. However, the restriction of the crack growth to stay within a plane imposes a very strong approximation to the natural crack growth. It has also been noticed that the manipulation of existing elements can result in a final mesh that includes somewhat distorted elements, see Fig. 2. The absence of a homogenous element distribution may influence the results. A further description

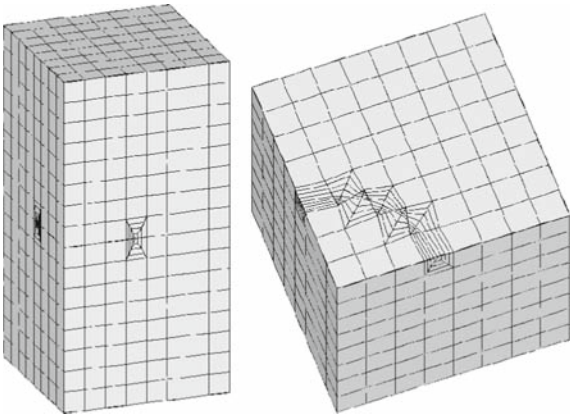

Fig. 2 The pure hexahedral mesh may hold distorted elements at the crack front as a result of the mesh manipulation

of the method can be found in (Dhondt 1998, 1999, 2005).

6 The combined element approach

The principal aim of this method is to eliminate any constraints on the crack growth so that the evolution can be represented naturally. The program should be free to choose its propagation direction according to the prevailing stress field. Additionally, independent of which fracture criterion is used, a homogenous structured mesh along and about the crack front is strived for. Since the crack front for almost all realistic applications will bend and curve, the structured mesh will take the shape of an arbitrary tube.

Not only does the structured tube mesh simplify the book-keeping but it also yields the most accurate results if the correct elements are assigned. This is important no matter which meshing method is applied. Since the crack growth calculations are directly depending on the stress field in the tube, the tube has to be regarded to constitute the core of the analysis.

Once the tube is generated, the second step is to mesh the remaining part of the structure without any user interaction. Tetrahedral elements are required for this purpose since this is the only element type that so far has shown proven the ability to mesh arbitrary domains. For this purpose the external software NETGEN (Schöberl 1997) is used.

At this point two meshes have been generated independently and are thus separate without any common elements or nodes. The dissimilar meshes are connected

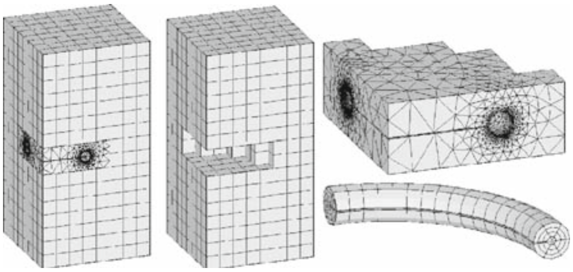

Fig. 3 An assembly of separate meshes result in a cracked mesh by the combined element method

through linear multiple point constraint (MPC) equations. The method is further described in (Bremberg and Dhondt 2008). Due to the lack of a perfect fit of nodes and elements, boundary and initial conditions have to be extrapolated and interpolated in order to fit the cracked mesh. This is easy for temperature fields but is non-trivial for more complex boundary conditions such as distributed loads and MPCs. Attempts have been made to resolve this matter but complications remain. A proposed solution to alleviate this problem is to keep the whole reference mesh intact with exception of a region enclosing the crack faces. This requires that the above described method is extended with a couple more operations. First, the region in the reference mesh that encloses the crack surfaces is identified. The cracked mesh is generated based on the selected elements rather than the complete input mesh. Finally, the cracked mesh replaces the selected mesh region and the remaining reference mesh and the cracked mesh are connected by MPCs. If it is assumed that the crack is located not too close to any prescribed boundary conditions, this method keeps the prescribed boundary conditions intact. This way only temperature, residual stresses and material parameters have to be mapped to the cracked mesh. The assembled cracked mesh is illustrated in Fig. 3.

7 Three example specimens

Three specimens are investigated in order to evaluate the two methods. These have been previously investigated using the quarter point element method and the modified virtual crack closure integral (Dhondt et al. 2001). The specimens and the corresponding loading have been chosen such that reference solutions are available in the literature (Murakami 1987). The loads

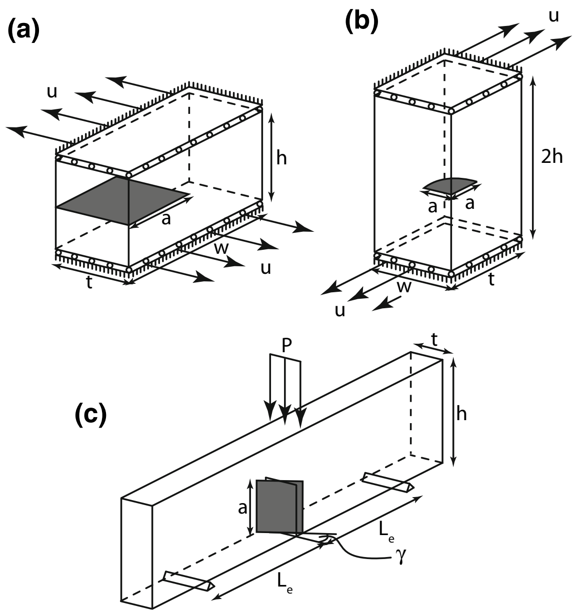

Fig. 4 Specimen geometries and loading for (**a**) a SEN specimen, (**b**) a QCCC specimen and (**c**) a 3PB specimen

and geometric specifications for the three specimens are given in Fig. 4 and Table 1.

The single edge notch (SEN) and quarter circular corner crack (QCCC) specimens are used to compare the SIF distributions between the pure element (PE) approach and the combined element (CE) approach. Normalized SIFs are computed for the two specimens using both methods in order to determine how well these results coincide with the reference solutions. The intention is to make sure that the combined element approach yields correct results for mixed mode loading. In addition, the SIFs and the equivalent SIF are compared to the deflection angle.

The three point bend (3PB) specimen, equipped with a crack inclined to the mid-plane, is used to perform crack growth computations for the MPS criterion. The example does not exhibit as strong mixed-mode loading as the SEN and QCCC specimens. Such strong mixed-mode loading scenarios are exceptional. The 3PB specimen on the other hand is a popular approach to investigate mixed mode loading in a relatively simple fashion. Compared to many other specimens it requires only a very simple symmetric experimental set up.

Table 1 Geometrical parameters for the three specimens

		SEN	QCCC	3PB
Length	Le/mm	–	–	120
Height	h/mm	25	100	–
Width	w/mm	100	100	60
Thickness	t/mm	50	100	20
a/w		0.5	0.4	0.3
Angle	γ	–	–	$\frac{\pi}{4}$

8 Stress intensity factor distributions

8.1 SEN specimen

The SEN specimen is subjected to a prescribed Mode-III deformation, see Fig. 5. This is confirmed by the resulting SIF results for both approaches which coincide well with the reference solution, see Fig. 6a. Equivalent SIFs evaluated by the two criteria show the different results obtained for pure Mode-III loading at $s/|s| = 0.5$, see Fig. 6b. For $0.3 < s/|s| < 0.7$ there is a good agreement between the numerical methods and the empirical results. Closer to the free surface the results show an increasing deviation. This is explained by the contraction effect of the specimen due to the global deformation. Although pure shear displacement is prescribed it is evident that a Mode-II deformation is introduced close to the free boundary.

The coupling of Mode-II and Mode-III results in a decrease in Mode-III and a significant increase in Mode-II. This effect is explained by the twisting of the crack front region as a result of surface effects.

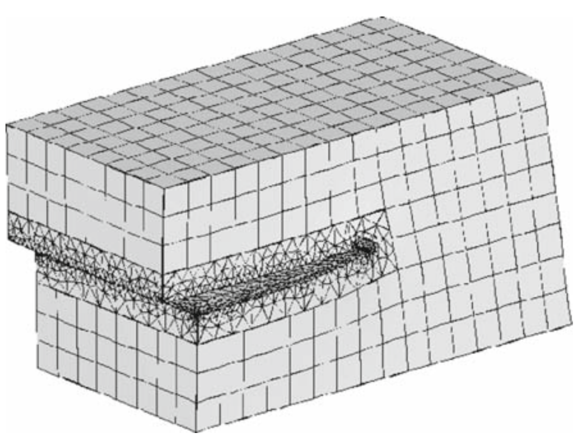

Fig. 5 The cracked SEN specimen illustrated with a magnified displacement

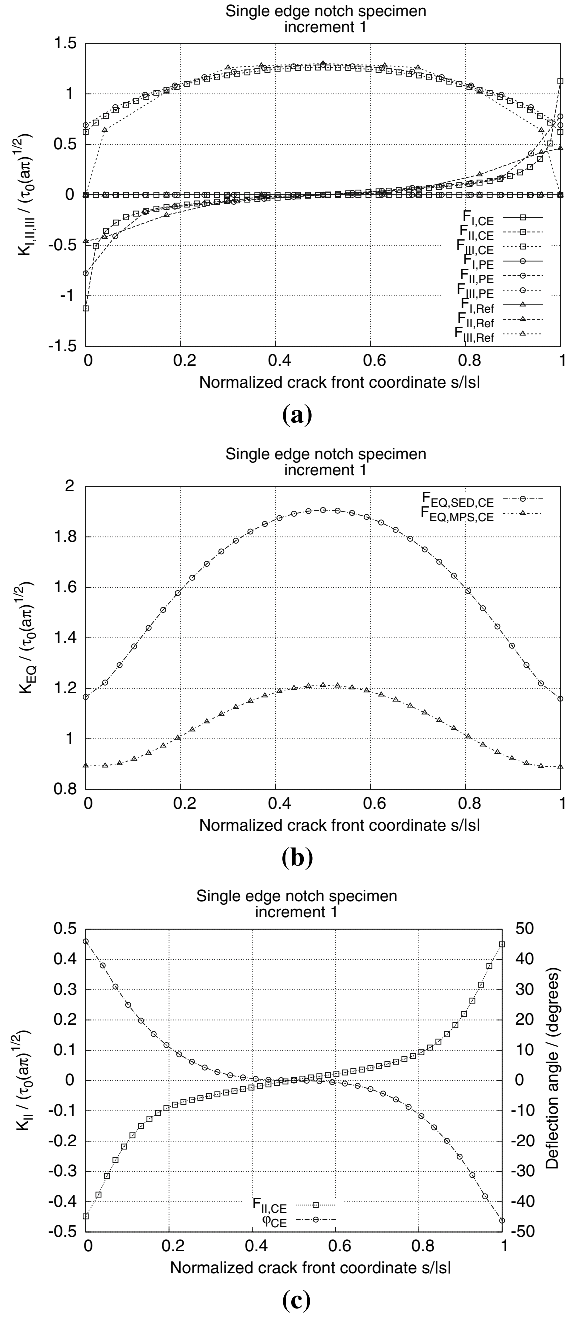

Fig. 6 Normalized values of (**a**) $K_{I,II,III}$, (**b**) K_{EQ} and (**c**) K_{II} and angle of deflection vs. normalized crack front coordinate for the single edge notch specimen

From the results it can be seen that the loading behaves symmetrically about the crack front center, except for Mode-II that changes sign, see Fig. 6c. The deflection angle is closely connected to the Mode-II loading and changes sign accordingly. This means that the crack would evolve in two different directions anti-symmetrically about the crack front centre. Any further computations with a tool that restricts the crack from growing out of plane clearly would not resemble the true crack growth. However, the SIFs for this first increment indeed give us an intuition of how the crack would evolve.

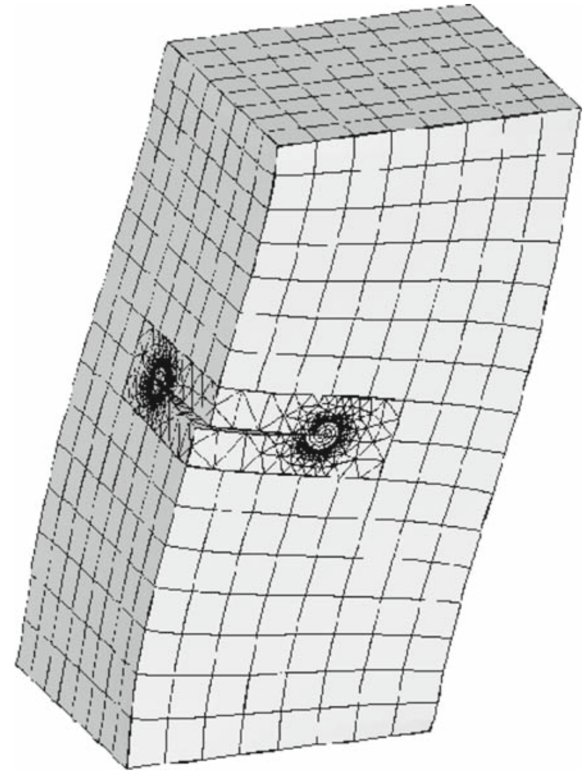

Fig. 7 The cracked QCCC specimen illustrated with a magnified displacement

8.2 QCCC specimen

The QCCC specimen is subjected to the same type of loading as the SEN specimen, see Fig. 7. It does however hold an important extra feature, a curved crack front. The results are expected to show a continuous transition from a pure Mode-III at one end of the crack front to a pure Mode-II at the other end, see Fig. 8a. This would probably be true unless there is a contraction and twisting effect close to the free surface. As for the SEN specimen, the equivalent SIFs point out the different results for pure Mode-III loading, see Fig. 8b. Figure 8c shows that the Mode-II contribution changes

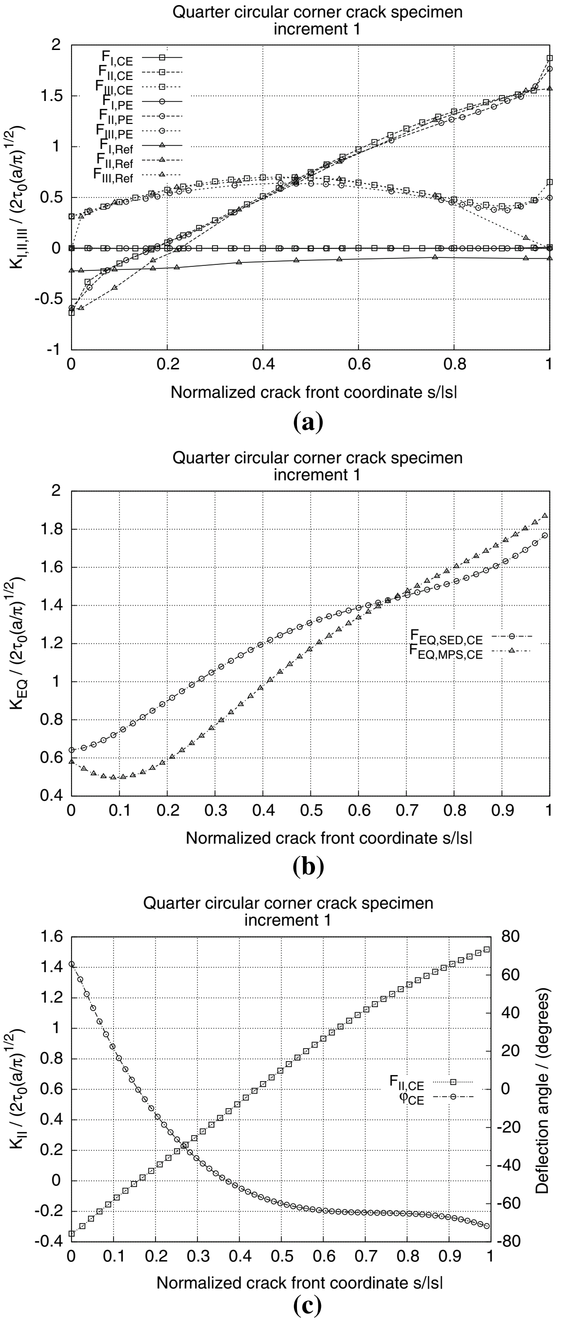

Fig. 8 Normalized values of (**a**) $K_{I,II,III}$, (**b**) K_{EQ} and (**c**) K_{II} and angle of deflection vs. normalized crack front coordinate for the quarter circular corner crack specimen

sign for the QCCC specimen as well, but not at the crack front centre. Due to the curvature of the crack front, the loading acts neither symmetrically nor anti-symmetrically about the crack front centre. Instead, the behaviour recorded for the SEN specimen becomes slightly shifted for the curved crack front. Consequently, the twisting behaviour of the crack front region yields a mode mixity that is now influenced by the characteristics of the twisting. A Mode-II twisting behaviour amplifies the effect of Mode-II and vice versa.

Analogously to the SEN specimen, the results coincide very well with the reference solution, except for the twisting behaviour and surface effects. The deflection angle behaves according to the Mode-II loading. The same type of crack growth deflection can evidently be expected for both specimens.

9 Mixed mode crack propagation

It is clear from the results for the SEN and QCCC specimens that the Mode-II loading has a strong influence on the crack front deflection. Both specimens represent loading cases where the Mode-I loading is limited. Although they constitute two very nice examples, such loading is rare in real life. Therefore, another example is examined for which a pronounced crack deflection can be expected, although not as extreme a case as the SEN and QCCC specimens.

The crack growth is predicted for 70 increments using the combined element approach together with the MPS fracture criterion. The cracked mesh after 70 increments is illustrated by Fig. 9. It is clearly visible how the crack has grown out of plane and has changed the direction of its crack front. A study of the resulting SIF distributions reveals how the crack slowly

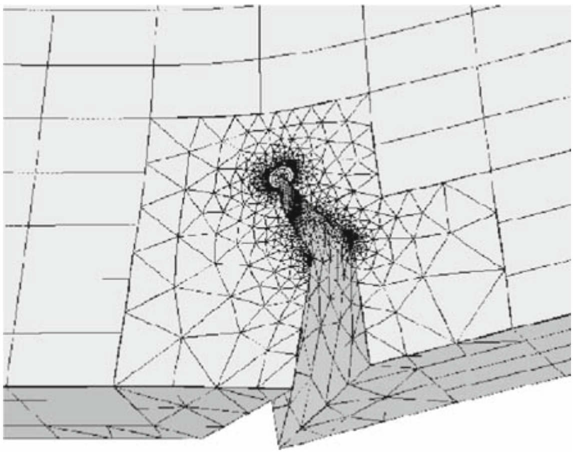

Fig. 9 The cracked 3PB specimen illustrated with a magnified displacement

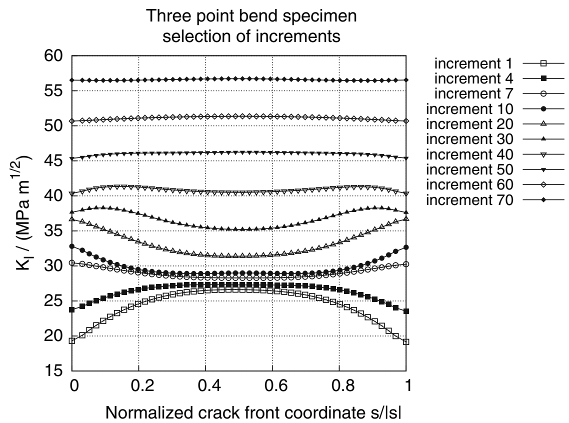

(a)

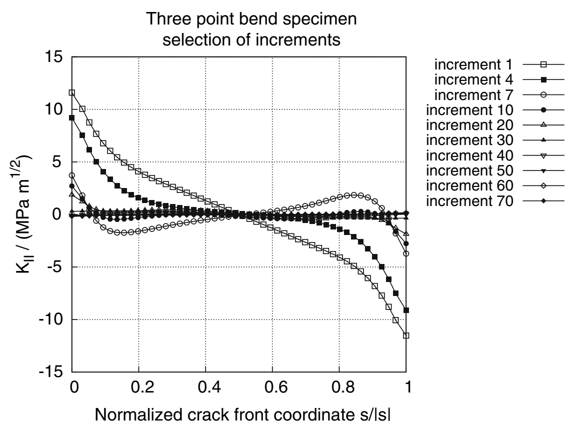

(b)

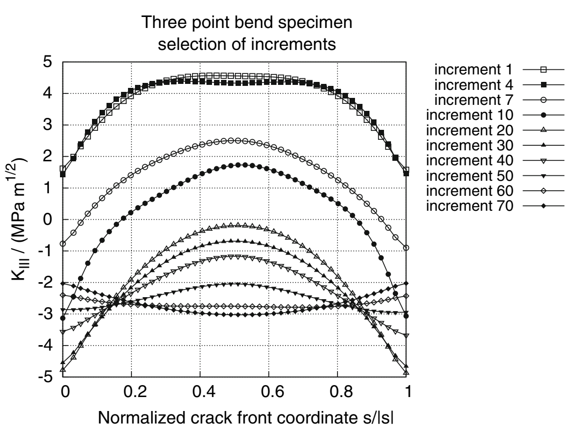

(c)

Fig. 10 (**a**) K_I, (**b**) K_{II} and (**c**) K_{III} along the crack front for a selection of increments

evolves towards a state of pure tension. The first increments show a distinct mixed mode loading that quickly decreases. It is worth pointing out that the crack rapidly grows out of plane as the KI, KII and KIII values are of

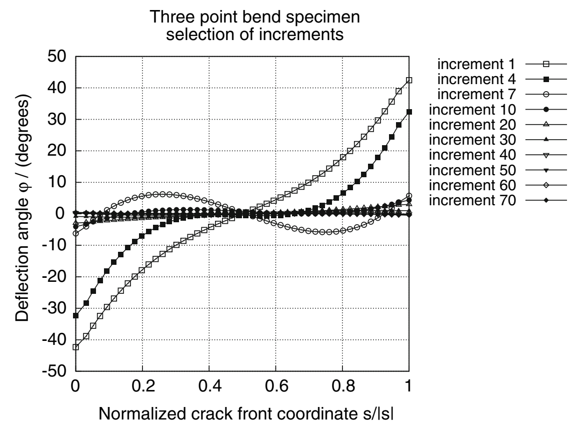

(a)

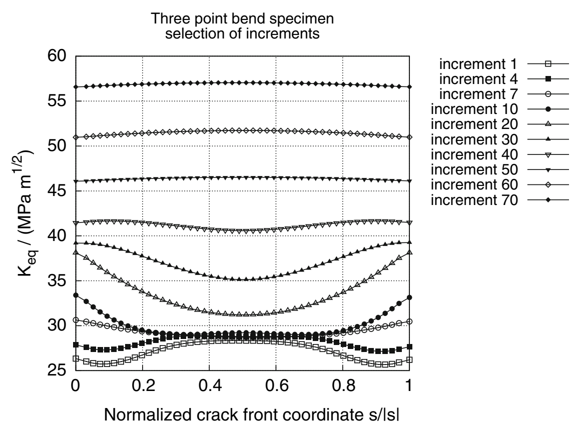

(b)

Fig. 11 (**a**) Angle of deflection and (**b**) equivalent SIF for a selection of increments

the same magnitude. The deflection immediately influences the Mode-I part that develops into the clearly dominating loading mode. Figure 10 shows how the SIFs change as the crack evolves.

Once the crack growth at the centre of the crack front slows down as it reaches an almost pure tension loading state, the remaining parts of the crack front exhibit the most crack growth as they catch up. After approximately 40 increments the crack front is exposed to a relatively homogenous loading and no further exciting phenomena can be expected to occur. Instead, the crack continues to grow and the mode mixity further decreases. Figure 11a reveals that the crack deflection acts anti-symmetrically about the crack front centre. Due to the deflection angle, the crack grows in a twisting path as if a torque were applied to the crack front centre and it eventually grows into a pure Mode-I loading. Computed equivalent SIFs nearly coincide with K_I after 70 increments.

10 Conclusion

From the investigation presented it can be concluded that the approach based on a combination of element types shows promising results. Results for the SEN and QCCC specimens agree well with empirical recordings for both the pure element approach and the reference solution. Significant deviation can be found close to the free surfaces for both numerical methods compared to the reference solution. This is expected to be a result from contraction and twisting effects. Whether or not the deviation is due to a limitation in the numerical procedures or a lack in the empirical recordings needs to be further investigated.

A comparison between the resulting crack propagation, SIF distributions and deflection angles for the 3PB specimen shows that the mode mixity strongly influences the crack growth.

The results encourage further development of the combined element approach, study of fracture criteria and growth laws.

References

BEASY (2007) BEASY V10r7 Documentation. C.M. BEASY Limited, 2007

Brebbia CA (1978) The boundary element method for engineers. Pentech Press, London

Bremberg D, Dhondt G (2008) Automatic crack-insertion for arbitrary crack growth. Eng Frac Mech 75:404–416

Chanel B, Dhondt G (2007) Verallgemeinerung des MTU 3-D Rissfortschrittskriteriums auf anisotrope materialien, 39. Tagung DVM-Arbeitskreis Bruchvorgnge, Dresden, 13–14 Feb 2007

Cicilino AP, Aliabadi MH (1999) Three-dimensional boundary element analysis of fatigue crack growth in linear and non-linear fracture problems. Eng Frac Mech 63:713–733

Citarella R, Buchholz FG (2008) Comparison of crack growth simulation by DBEM and FEM for SEN-specimens undergoing torsion or bending loading. Eng Frac Mech 72:489–509

Dhondt G (1993) General behaviour of collapsed 8-node 2-D and 20-node 3-D isoparametric elements. Int J Num Meth Eng 36:1223–1243

Dhondt G (1998) Automatic 3-D mode I crack propagation calculation with finite elements. Int J Num Meth Eng 41:739–757

Dhondt G (1999) Automatic Three-dimensional cyclic crack propagation predictions with finite elements at the design stage of an aircraft engine. In: RTO AVT Symposium on design principles and methods for aircraft gas turbine engines. 11–15 May 1998. Toulouse, France, RTO MP-8, pp 33-1–33-8

Dhondt G (2005) Cyclic crack propagation at corners and holes. Fatigue Frac Eng Mater Struct 28:25–30

Dhondt G, Chergui A, Buchholz FG (2001) Computational fracture analysis of different specimens regarding 3D and mode coupling effects. Eng Frac Mech 68:383–401

Forman RG et al (1988) Development of the NASA/FLAGRO computer program. In: Read DT, Read RP (eds) Fracture mechanics: eighteenth symposium, ASTM STP 945. American society for testing and materials. Philadelphia, PA, pp 781–803

Mi Y, Aliabadi MH (1992) Dual boundary element method for three-dimensional fracture mechanics analysis. Eng anal Boundary Elem 1:161–171

Murakami Y (ed) (1987) Stress intensity factors handbook. Pergamon Press, Oxford

NASCRAC (1989) Theory manual. Failure analysis associates. Palo Alto, CA

Paris PC, Erdogan F (1963) A critical analysis of crack propagation laws. J Basic Eng 85:528–534

Paris PC, Gomez MP, Anderson WE (1961) A rational analytical theory of fatigue. Trend Eng 13:9–14

Richard HA, Buchholz FG, Kullmer G, Schllmann M (2003) 2D- and 3D-mixed mode fracture criteria. Key Eng Mater 251–252:251–260

Riddell WT, Ingraffea AR, Wawrzynek PA (1997) Experimental observations and numerical predictions of three-dimensional fatigue crack propagation. Eng Frac Mech 58:293–310

Schöllmann M, Fulland M, Richard HA (2003) Development of a new software for adaptive crack growth simulations in 3D structures. Eng Frac Mech 70:249–268

Schöberl J (1997) NETGEN—An advancing front 2D/3D-mesh generator based on abstract rules. Comp Vis Sci 1:42–52

Timbrell C, Cook G (1997) 3-D FE fracture mechanics analysis for industrial applications. Zentech International Limited, UK. Seminar: "Inelastic finite element analysis", Institute of Mechanical Engineering, London, October 14, 1997

Wawrzynek PA, Martha LF and Ingraffea AR (1988) A computational environment for the simulation of fracture processes in three dimensions. In: Rosakis AJ et al (ed) Analytical, numerical and experimental aspects of three dimensional fracture processes. ASME AMD 91:321-327

Zienkiewicz OC (1971) The finite element method in engineering science. McGraw Hill, London